Imaging as an mTOR biomarker: Watanabe and colleagues review current knowledge about mammalian target of rapamycin signaling, function, inhibitors, and therapeutic targets and look at the potential for PET in visualizing and elucidating mTOR network complexity and function. . . *Page 497*

Lognormal uptake of radioactivity: Zanotti-Fregonara and Hindié provide perspective on a strategy to compensate for heterogeneity in radioactivity distribution at the cellular level in predicting absorbed dose and biologic response. . . . *Page 501*

SPECT and chronic Chagas cardiomyopathy: Miranda and colleagues investigate associations between cardiac sympathetic denervation and sustained ventricular tachycardia in patients with cardiac complications from Chagas disease. . . . . *Page 504*

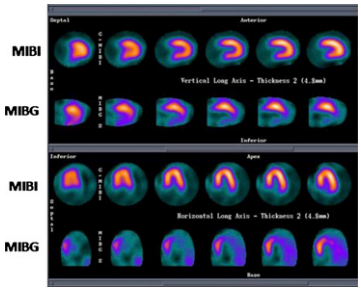

SPECT and PET in stroke: Chida and colleagues compare central benzodiazepine receptor binding potential and cerebral blood flow SPECT images with PET oxygen extraction images in patients with chronic cerebral occlusive disease. . . . . *Page 511*

Imaging in neuroblastoma: Papathanasiou and colleagues evaluate the diagnostic performance and prognostic significance of ^{18}F-FDG PET/CT in comparison with ^{123}I-MIBG imaging in patients with high-risk neuroblastoma. . . . . *Page 519*

Antipsychotic receptor occupancy: Catafau and colleagues assess human striatal dopamine receptor 2 and 5-HT$_{2A}$ occupancy of the antipsychotic SB-773812 as an indicator of brain penetration, binding to target receptors, and receptor occupancy over time. . . . . *Page 526*

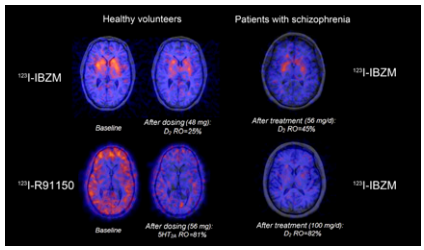

PET and macromolecular uptake: Pryma and colleagues explore correlations between quantification of radiolabeled macromolecular uptake in tumors determined in vivo using PET/CT and in vitro using autoradiography and γ-counting of tumor tissue. . . . . *Page 535*

Multiagent PET in sarcoma: Eary and colleagues describe a 6-agent protocol with which patients with soft-tissue sarcoma were imaged in a single session, yielding data on tumor proliferation, drug resistance activity, and tissue hypoxia. . . . *Page 541*

^{18}F-FDG pituitary gland uptake: Hyun and colleagues report on the frequency and clinical significance of incidental pituitary uptake on whole-body ^{18}F-FDG PET/CT. . . . . *Page 547*

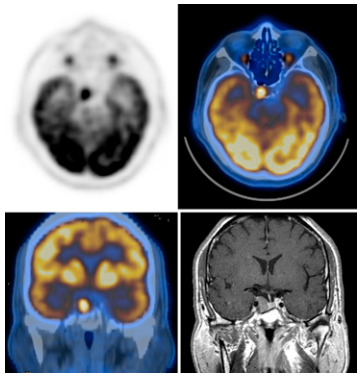

Sentinel node imaging in testicular cancer: Brouwer and colleagues assess the utility of SPECT/CT and real-time intraoperative imaging with a portable γ-camera for laparoscopic sentinel node localization in stage 1 testicular cancer. . . . . *Page 551*

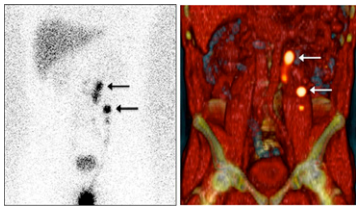

Bispecific antibody pretargeting: Karacay and colleagues detail preparation of and initial studies with a ^{68}Ga-labeled hapten peptide with promise for immuno-PET applications. . . . . *Page 555*

Imaging treatment-induced cardiotoxicity: de Geus-Oei and colleagues provide an educational overview of past, current, and promising radiopharmaceuticals and scintigraphic techniques used to evaluate cardiotoxicity resulting from anticancer agents. . . *Page 560*

Silicon photomultiplier PET: Kwon and colleagues describe the development of and feasibility studies with a small-animal PET system equipped with silicon photomultipliers and lutetium gadolinium oxyorthosilicate crystals. . . . . *Page 572*

Interferon ^{68}Ga small-animal PET: Hanin and colleagues report on studies designed to determine whether interferon-α can increase tumor uptake in peptide receptor radionuclide therapy in a small-animal model of neuroendocrine tumors. . . . . *Page 580*

Universal ^{68}Ga labeling of proteins: Wängler and colleagues present simplified labeling chemistry to attach the versatile radionuclide ^{68}Ga to proteins for use in the development of a variety of PET agents. . . . . *Page 586*

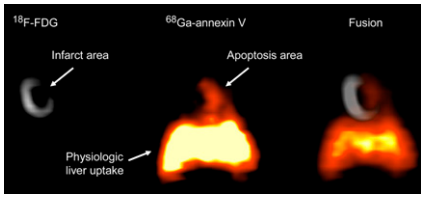

^{18}F-C2A-GST PET in lung cancer: Wang and colleagues describe the development of ^{18}F-labeled C2A-glutathione-S-transferase as a molecular imaging probe for detection of apoptosis and use it to assess response to paclitaxel chemotherapy in a rabbit model. . . . . ***Page 592***

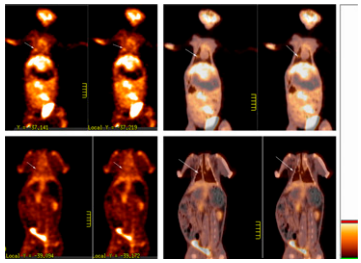

Inflammatory pain imaging: Jacobson and colleagues report on the use of ^{18}F-PC-10 PET to image prokineticin receptor 1 as a biomarker of inflammation and inflammation-based pain. . . . . ***Page 600***

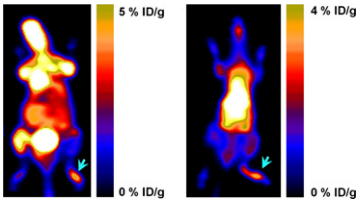

Targeting melanoma: Guo and colleagues look at the effects of amino acid linkers on the melanoma-targeting and pharmacokinetic properties of three ^{111}In-labeled α-melanocyte–stimulating hormone peptides and describe the potential for both imaging and therapy. . . . . ***Page 608***

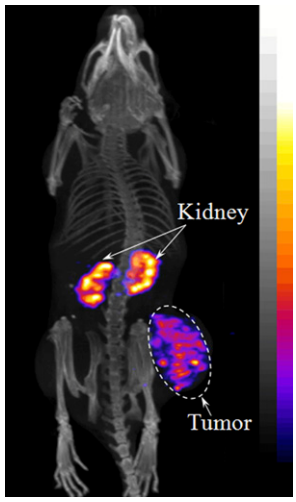

^{18}F-flurpiridaz flow quantification: Sherif and colleagues hypothesize that myocardial retention and uptake values based on late uptake of this PET tracer can provide accurate estimates of myocardial flow reserve for simplified quantification after tracer injection outside the PET scanner. . . . . ***Page 617***

Phenotypic influence on EPR effect: Heneweer and colleagues investigate the influence of different tumor phenotypes on the enhanced permeability and retention effect in targeted macromolecular radiotracers. . . . . ***Page 625***

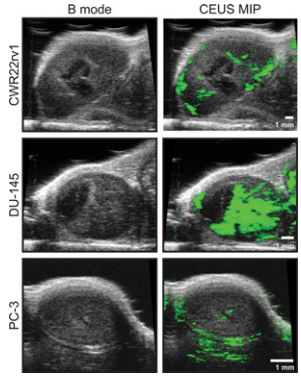

Simplified kinetic analysis in ^{18}F-FDG PET: Hapdey and colleagues extend the simplified kinetic analysis technique for estimating glucose metabolic rate, allowing for a variety of arterial input function curves and accounting for unmetabolized tracer in tumors. . . . . ***Page 634***

Radiochemotherapy cocktail design: Akudugu and colleagues describe a technique using changes in the value of the lognormal shape parameter and slope of cellular drug uptake curves to rapidly screen radiopharmaceuticals and other agents for more effective chemotherapeutic cocktails. . . . . ***Page 642***

Training molecular imaging scientists: Zinn and colleagues provide a consensus report on the recommended content of a molecular imaging curriculum based on the core competencies and the integrative nature of the field. . . . . ***Page 650***

ON THE COVER

ImmunoPET may be useful in quantitatively assessing antigen targeting by antibody-based therapies, allowing for noninvasive interrogation of all sites of disease over time. In these images of patients with clear cell renal cancer, antigen distribution is heterogeneous within the primary tumor but relatively homogeneous within metastatic nodes.

See page 537.